

Astroglial potassium clearance contributes to short-term plasticity of synaptically evoked currents at the tripartite synapse

Jérémie Sibille^{1,2}, Ulrike Pannasch¹ and Nathalie Rouach¹

¹Neuroglial Interactions in Cerebral Physiopathology, Center for Interdisciplinary Research in Biology, Collège de France, Centre National de la Recherche Scientifique UMR 7241, Institut National de la Santé et de la Recherche Médicale U1050, 75005 Paris, France

²Université Paris Diderot, Sorbonne Paris Cité, 75013 Paris, France

Key points

- Astrocytes, active players in neurotransmission, display complex membrane ionic responses upon neuronal activity.
- However, the nature, plasticity and role of the activity-dependent astroglial currents on synaptic plasticity remain unclear in the hippocampus.
- We here demonstrate, using simultaneous electrophysiological recordings of hippocampal neurons and astrocytes, that the complex astroglial current induced synaptically is dominated (80%) by potassium entry through $K_{ir}4.1$ channels and also includes, in addition to the glutamate transporter current, a small residual current, partially mediated by GABA transporters and $K_{ir}4.1$ -independent potassium channels.
- These synaptically evoked astroglial currents exhibit differential short-term plasticity patterns, and astroglial potassium uptake mediated by $K_{ir}4.1$ channels down-regulates hippocampal short-term plasticity.
- This study establishes astrocytes as integrators of excitatory and inhibitory synaptic activity, which may, through dynamic potassium handling, define the signal-to-noise ratio essential for specific strengthening of synaptic contacts and synchronization of neuronal ensembles, a prerequisite for learning and memory.

Abstract Astroglial processes enclose ~60% of CA1 hippocampal synapses to form the tripartite synapse. Although astrocytes express ionic channels, neurotransmitter receptors and transporters to detect neuronal activity, the nature, plasticity and impact of the currents induced by neuronal activity on short-term synaptic plasticity remain elusive in hippocampal astrocytes. Using simultaneous electrophysiological recordings of astrocytes and neurons, we found that single stimulation of Schaffer collaterals in hippocampal slices evokes in stratum radiatum astrocytes a complex prolonged inward current synchronized to synaptic and spiking activity in CA1 pyramidal cells. The astroglial current is composed of three components sensitive to neuronal activity, i.e. a long-lasting potassium current mediated by $K_{ir}4.1$ channels, a transient glutamate transporter current and a slow residual current, partially mediated by GABA transporters and $K_{ir}4.1$ -independent potassium channels. We show that all astroglial membrane currents exhibit activity-dependent short-term plasticity. However, only the astroglial glutamate transporter current displays neuronal-like dynamics and plasticity. As $K_{ir}4.1$ channel-mediated potassium uptake contributes to 80% of the synaptically evoked astroglial current, we investigated in turn its impact on short-term synaptic plasticity. Using glial conditional $K_{ir}4.1$ knockout mice, we found that astroglial potassium uptake reduces synaptic responses to repetitive stimulation

and post-tetanic potentiation. These results show that astrocytes integrate synaptic activity via multiple ionic channels and transporters and contribute to short-term plasticity in part via potassium clearance mediated by $K_{ir}4.1$ channels.

(Received 4 July 2013; accepted after revision 27 September 2013; first published online 30 September 2013)

Corresponding author N. Rouach: Neuroglial Interactions in Cerebral Physiopathology, Collège de France, CIRB, CNRS UMR 7241, INSERM U1050, 11, place Marcelin Berthelot, 75005 Paris, France. Email: nathalie.rouach@college-de-france.fr

Abbreviations ACSF, artificial cerebrospinal fluid; AMPAR, AMPA receptor; AP, action potential; CPP, (RS)-3-(2-carboxypiperazin-4-yl)propyl-1-phosphonic acid; $Cx30^{-/-}Cx43^{-/-}$, $Cx30^{-/-}Cx43^{fl/fl}:hGFAP-Cre$ mice; EPSC, excitatory postsynaptic current; EPSP, excitatory postsynaptic potential; fEPSP, field excitatory postsynaptic potential; GAT, GABA transporter; GDP- β -S, guanosine 5'-[β -thio]diphosphate; GLT, glutamate transporter; GluR, glutamate receptor; I_{GluT} , astroglial glutamate transporter current; I_K , astroglial potassium current; I_m , astroglial membrane current; I_{res} , astroglial residual current; I_{tot} , total astroglial current; $I-V$, current-voltage; K_{ir} channel, inward rectifier potassium channel; $K_{ir}4.1$ cKO, $K_{ir}4.1^{fl/fl}:hGFAP-Cre$ mice; K_{2p} , two pore-domain potassium channel; LTP, long-term potentiation; 2-NBDG, 2-[N-(7-nitrobenz-2-oxa-1,3-diazol-4-yl)amino]-2-deoxyglucose; NMDAR, NMDA receptor; PTP, post-tetanic potentiation; TBOA, DL-threo- β -benzyloxyaspartic acid; TTX, tetrodotoxin; V_m , membrane potential; SCs, Schaffer collaterals.

Introduction

Recent data suggest that astrocytes play an important role in behavioural states and cognitive functions (Ben Achour & Pascual, 2012). Astrocytes integrate neuronal activity through their membrane channels, receptors and transporters, and can transmit information, in part, by complex calcium responses. Astroglial calcium signalling has been extensively studied, and is thought to represent their excitability. It is proposed to trigger the release of gliotransmitters (such as glutamate, ATP and D-serine) and to modulate neuronal activities (Nedergaard & Verkhratsky, 2012). In contrast, although glial membrane depolarization was the first activity-dependent signal identified (Orkand *et al.* 1966), the ionic responses of astrocytes received less attention, because of their slower time scale, the passive glial membrane properties and the lack of selective pharmacological tools to investigate their functional consequences. Nevertheless, neuronal activity induces in glial cells ionic currents with various components in different brain regions, such as potassium currents (Orkand *et al.* 1966; Karwoski *et al.* 1989; Meeks & Mennerick, 2007), glutamate and GABA transporter (GLT, GAT) currents (Bergles & Jahr, 1997; Diamond *et al.* 1998; Luscher *et al.* 1998; Goubard *et al.* 2011), or AMPA receptor (AMPA) currents in cerebellar Bergmann glia (Clark & Barbour, 1997; Bellamy & Ogden, 2005).

The role of these glial currents in neuroglial interactions and neurotransmission has been addressed by only a few studies. For instance, calcium entry through glutamate receptor 2 (GluR2)-lacking AMPARs in cerebellar Bergmann glia enables proper structural and functional neuroglial interactions. As a consequence, Bergmann glia tightly enclose nearly 70% of glutamatergic synapses to efficiently take up synaptically released glutamate (Iino

et al. 2001), and thereby control motor coordination (Saab *et al.* 2012). In addition, astroglial GLTs are crucial for maintaining low levels of extracellular glutamate, which otherwise spill over and activate extrasynaptic receptors, regulating release probability, and neighbouring synapses (Oliet *et al.* 2001; Huang *et al.* 2004; Piet *et al.* 2004; Filosa *et al.* 2009; Omrani *et al.* 2009). By such action, astroglial GLTs thus indirectly regulate excitatory transmission, and can protect against epileptic activity and excitotoxicity (Rothstein *et al.* 1996; Tanaka *et al.* 1997). Finally, potassium currents mediated by $K_{ir}4.1$ channels in glia regulate spontaneous excitatory synaptic currents and the early stage of long-term potentiation (LTP; Djukic *et al.* 2007).

Astrocytes, like neurons, exhibit several forms of plasticity, including a morphological plasticity of neuronal coverage during specific physiological conditions (Genoud *et al.* 2006; Oliet & Bonfardin, 2010), as well as a functional plasticity of neuronal-induced currents. In the cerebellum, currents evoked in Bergmann glia by parallel fibre stimulation exhibit activity-dependent short-term and long-term plasticity (Bellamy & Ogden, 2005, 2006), while in the hippocampus, astroglial potassium signals display LTP, like neuronal currents (Ge & Duan, 2007; Zhang *et al.* 2009). However, the nature, relative weight, short-term plasticity and role of the activity-induced astroglial currents in synaptic plasticity remain elusive in the hippocampus. Therefore, the aims of our study were: (1) to better characterize the different synaptically induced astroglial currents to systematically relate these astroglial responses to the simultaneously evoked neuronal responses; (2) to investigate whether the synaptically evoked astroglial currents display specific patterns of short-term plasticity; and (3) to determine in turn the impact of the major astroglial potassium current on hippocampal short-term synaptic plasticity.

Using dual electrophysiological recordings, we found that stimulation of Schaffer collaterals (SCs) elicits fast neuronal responses synchronized to a complex astroglial current, composed of three components, which exhibit short-term plasticity with different dynamics. The small astroglial residual current is partially mediated by GATs and $K_{ir}4.1$ -independent potassium channels. However, the synaptically evoked current in astrocytes is dominated by potassium entry through $K_{ir}4.1$ channels, which down-regulates hippocampal short-term synaptic plasticity. This suggests an important role for astrocytic $K_{ir}4.1$ channels on ambient potassium levels and pre-synaptic release.

Methods

Ethical approval

Experiments were carried out according to the guidelines of European Community Council Directives of 24 November 1986 (86/609/EEC) and of our local animal welfare committee (Center for Interdisciplinary Research in Biology in Collège de France), and conform to the principles of UK regulations as described in Drummond (2009). All efforts were made to minimize the number of used animals and their suffering.

Animals

Experiments were performed on the hippocampus of wild-type mice (C57BL6), $K_{ir}4.1$ fl/fl:hGFAP-Cre mice ($K_{ir}4.1$ cKO) (provided by K. D. McCarthy, University of North Carolina, USA), with conditional deletion of $K_{ir}4.1$ in glia (Djukic *et al.* 2007; Chever *et al.* 2010), as well as $Cx30^{-/-}$ Cx43fl/fl:hGFAP-Cre mice ($Cx30^{-/-}$ Cx43 $^{-/-}$, double knockout) (provided by K. Willecke, University of Bonn, Germany), with conditional deletion of $Cx43$ in astrocytes (Theis *et al.* 2003) and additional total deletion of $Cx30$ (Teubner *et al.* 2003), as previously described (Wallraff *et al.* 2006; Pannasch *et al.* 2011). Animals were killed by cervical dislocation and decapitated. For all analyses, mice of both sexes and littermates were used (16–25 days old).

Electrophysiology

Acute transverse hippocampal slices (300–400 μ m) were prepared as previously described (Pannasch *et al.* 2011) from 16–25-days-old wild-type mice, glial conditional $K_{ir}4.1$ knockout mice ($K_{ir}4.1$ fl/fl:hGFAP-Cre mice, $K_{ir}4.1^{-/-}$) (Djukic *et al.* 2007) and $Cx30^{-/-}$ Cx43 $^{-/-}$ (Pannasch *et al.* 2011). Slices were maintained at room temperature (21–23°C) in a storage chamber that was perfused with artificial cerebrospinal fluid (ACSF)

containing (in mM): 119 NaCl, 2.5 KCl, 2.5 CaCl₂, 1.3 MgSO₄, 1 NaH₂PO₄, 26.2 NaHCO₃ and 11 glucose, saturated with 95% O₂ and 5% CO₂, for at least 1 h prior to recording. Slices were transferred to a submerged recording chamber mounted on an Olympus BX51WI microscope equipped for infra-red differential interference contrast microscopy and were perfused with ACSF at a rate of 1.5 ml · min⁻¹ at room temperature. All experiments were performed in the presence of picrotoxin (100 μ M), and a cut was made between CA1 and CA3 to prevent the propagation of epileptiform activity. Dual electrophysiological recordings of CA1 pyramidal neurons (extracellular or whole-cell patch clamp) and astrocytes (whole-cell patch clamp) were performed, unless otherwise stated. Evoked postsynaptic or astrocytic responses were induced by stimulating SCs (0.05 Hz) in CA1 stratum radiatum with ACSF-filled glass pipettes (300–700 k Ω). Field excitatory postsynaptic potentials (fEPSPs) were recorded in stratum radiatum with glass pipettes (4–6 M Ω) filled with ACSF. To characterize the astroglial responses, we performed whole-cell recordings from visually identified stratum radiatum astrocytes, exhibiting typical morphological and electrophysiological properties. Stratum radiatum astrocytes were identified by their small soma (5–10 μ m), low membrane resistance and resting membrane potentials (\approx -80 mV), passive membrane properties (linear I–V relationship), lack of action potentials and extensive gap junctional coupling (Fig. 1A). Somatic whole-cell recordings were obtained from visually and electrophysiologically identified CA1 pyramidal cells and stratum radiatum astrocytes, using 4–6 M Ω glass pipettes filled with (in mM): 105 potassium gluconate, 30 KCl, 10 Hepes, 10 phosphocreatine, 4 MgATP, 0.3 GTP-Tris and 0.3 EGTA (pH 7.4, 280 mosmol l⁻¹); or for synaptic activity recordings, 115 mM CsMeSO₃, 20 mM CsCl, 10 mM Hepes, 2.5 mM MgCl₂, 4 mM Na₂ATP, 0.4 mM NaGTP, 10 mM sodium phosphocreatine, 0.6 mM EGTA, 0.1 mM spermine and 5 mM QX314 (pH 7.4, 280 mosmol l⁻¹). In voltage-clamp recordings, astrocytes and neurons were clamped at -80 and -60 mV, respectively. Membrane and series resistances were continuously monitored. Cells were discarded when the resting membrane potential varied by more than 10% or when series resistance varied by more than 20%. Whole cell series resistances ranged from 5 to 15 M Ω . Stimulus artifacts were blanked in sample traces. For intercellular coupling experiments, the internal solution contained dextran tetramethylrhodamine (1 mg · ml⁻¹) to identify the recorded astrocyte, as well as 2-[N-(7-nitrobenz-2-oxa-1,3-diazol-4-yl)amino]-2-deoxyglucose (2-NBDG; 2 mg · ml⁻¹), which diffused passively in astrocytic networks. The field recording pipette was placed 10–100 μ m away from the recorded astrocyte. Postsynaptic ionotropic GluR activity and subsequent astroglial potassium currents (I_K) were

blocked by kynurenic acid (2–5 mM), which has no direct effect on hippocampal passive astrocytes connected by gap junctions that we recorded from, because they lack AMPARs (Matthias *et al.* 2003; Wallraff *et al.* 2004; Bergles *et al.* 2010). Astrocytic I_K were isolated by subtracting the kynurenic acid-insensitive component from the total current (Fig. 2A). Glutamate transporter currents from astrocytes (I_{GluT}) were blocked by DL-threo- β -benzyloxyaspartic acid (TBOA; 200 μM). Astroglial I_{GluT} were isolated by subtracting the TBOA insensitive slow residual current component (I_{res}) from the response in the presence of kynurenic acid (Fig. 2A). Neuronal paired-pulse facilitation and astroglial summation were induced by delivery of two stimuli at different interpulse intervals (20–2000 ms). Prolonged repetitive stimulation was performed at 10 Hz for 30 s. Post-tetanic potentiation was induced by stimulation at 100 Hz for 1 s in the presence of 10 μM (RS)-3-(2-carboxypiperazin-4-yl)-propyl-1-phosphonic acid (CPP). Paired pulse ratios of evoked signals (fEPSPs and astroglial currents) were measured by dividing the peak amplitude of the second response by that of the first response, both measured with reference to the initial resting baseline (I_{rest}), taken before the first stimulation (Suppl. Fig. S1). Responses to repetitive (10 Hz, 30 s) or tetanic (100 Hz, 1 s) stimulation (neuronal fEPSP slope, and astroglial peak current amplitude measured to the initial resting baseline (I_{rest}) taken before the first stimulation) were binned (bin size 1.2 s and 100 ms, respectively) and normalized to mean baseline response (I_0) measured at 0.066 Hz before repetitive or tetanic stimulation (Fig. S1). Quantification of fast responses (fEPSPs and astroglial I_{GluT}) evoked repetitively, performed by measuring peak amplitudes with reference to pre-stimuli baselines, taken just before each stimulation, or to initial resting baseline (I_{rest}), taken before the first stimulation, leads to the same result because both baselines are the same in this case (Fig. S1). Recordings were acquired with Axopatch-1D amplifiers (Molecular Devices, Sunnyvale, CA, USA), digitized at 10 kHz, filtered at 2 kHz, stored and analysed on computer using Pclamp9, Clampfit9 (Molecular Devices) and MatLab software (MathWorks, Natick, MA, USA). All data are expressed as mean \pm standard error of the mean (SEM). Statistical significance for within-group comparisons was determined by one-way repeated-measures analyses of variance (ANOVAs; followed by Dunnett's post-test), whereas unpaired or paired *t* tests were used for between-group comparisons. Salts, picrotoxin, quinine, barium and guanosine 5'-[β -thio]diphosphate (GDP- β -S) were obtained from Sigma (St Louis, MO, USA), and all other chemicals were from Tocris (Bristol, UK).

Results

Synaptically evoked synchronous responses of hippocampal CA1 pyramidal cells and astrocytes

To directly compare the astroglial and excitatory neuronal responses evoked synaptically in the CA1 area of the hippocampus, we systematically performed synchronous recordings of fEPSPs and astrocytic membrane currents, evoked by SC stimulation in the presence of picrotoxin (100 μM ; Fig. 1B). Dual recordings in response to single stimulation of neuronal afferences revealed partially correlated activities in astrocytes and pyramidal neurons. The complex astroglial response consisted of: a fast outward current, reflecting fEPSPs generated by adjacent pyramidal cells (1 ms time lag), followed by a slow inward current, persisting several seconds after termination of the neuronal response (750 ms time lag; Fig. 1E) as previously reported (Bergles & Jahr, 1997; Diamond *et al.* 1998; Luscher *et al.* 1998; Ge & Duan, 2007; Henneberger *et al.* 2010; Henneberger & Rusakov, 2012). Astroglial inward currents of ~ -30 pA (-29.8 ± 1.3 pA, $n = 6$), evoked by moderate single SC stimulation, induced astrocytic membrane depolarizations of ~ 1.5 mV (1.6 ± 0.4 mV, $n = 6$; Fig. 1C, D). However, both responses had similar kinetics (time of peak, current: 0.46 ± 0.23 s, depolarization: 0.5 ± 0.16 s; decay time, current: 4.6 ± 0.57 s, depolarization: 4.26 ± 0.24 s, correlation coefficient: -0.98 at 187 ms time lag, $n = 6$; Fig. 1D), suggesting that electrotonic filtering is not responsible for the different kinetics of the synaptically evoked neuronal and astroglial responses.

To evaluate the strength of neuron to glia transmission, we first compared the amplitude of the presynaptic fibre volley (input), reflecting action potentials generated in the presynaptic fibres, to that of the astroglial current (output). The astrocytic response increased linearly with the neuronal input over a wide range of inputs (fibre volley amplitude tested from 0.1 to 0.9 mV; Fig. 1F). We then performed simultaneous whole-cell recordings from CA1 pyramidal neurons and astrocytes to determine the postsynaptic responses associated with the astrocytic currents recorded in the input–output curve (Fig. 1F). We thus investigated excitatory postsynaptic current (EPSC) size, paired-pulse ratio and spiking of the postsynaptic cells for defined amplitudes of astroglial currents evoked by extracellular stimulation. Stimulation of SCs to induce astrocytic currents from 10 to 60 pA evoked in neighbouring postsynaptic CA1 pyramidal cells EPSCs in the range of 124 ± 37 to 442 ± 80 pA ($n = 5$, Fig. 1G, H), as well as corresponding EPSPs and action potential firing (from 0.28 ± 0.1 to 2.62 ± 0.5 evoked action potentials, $n = 5$, Fig. 1I, J). In dual whole cell recording conditions where SCs were stimulated moderately to induce an

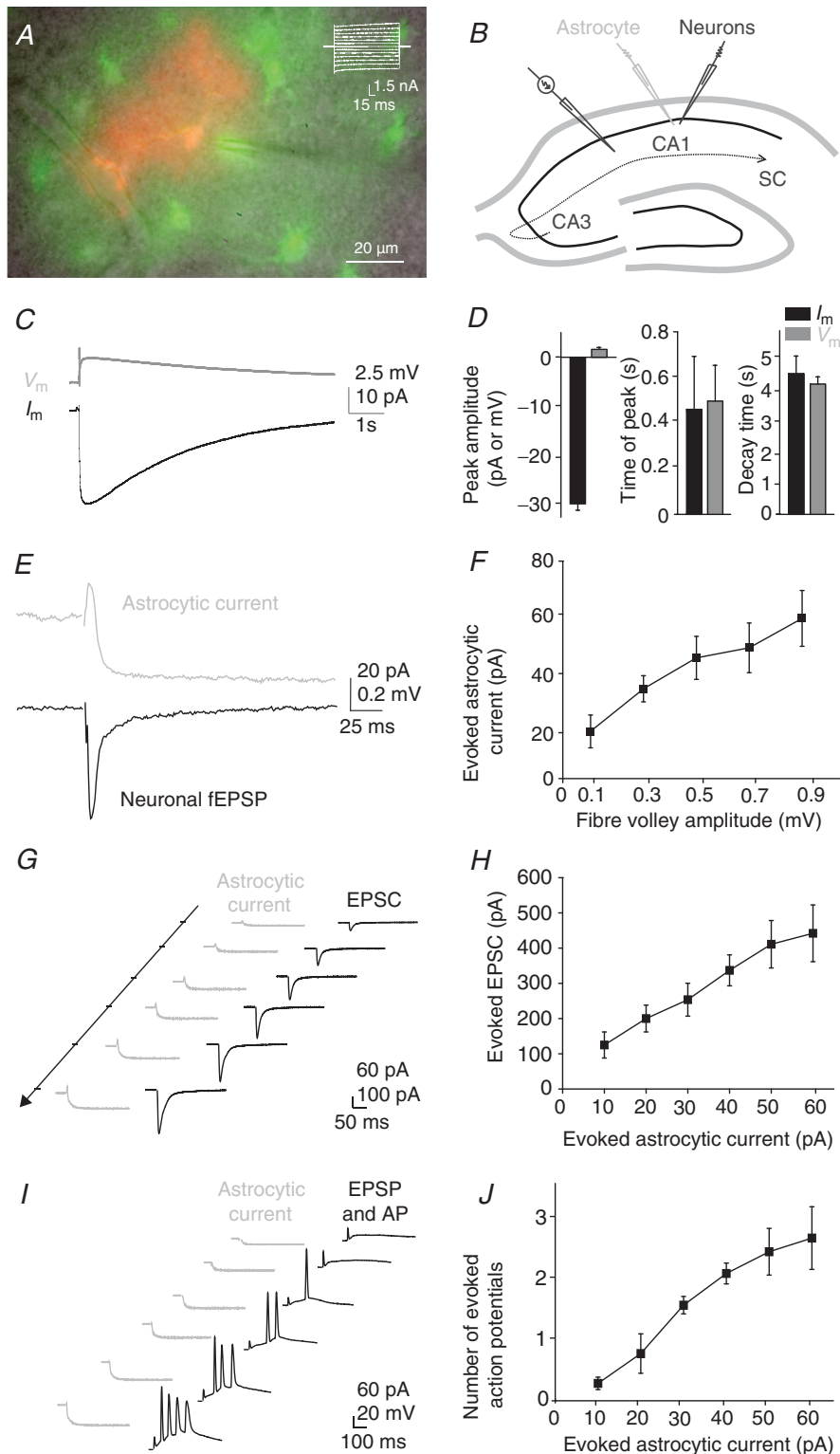


Figure 1. Patterns of synchronous responses evoked synaptically in hippocampal CA1 pyramidal cells and astrocytes

A, sample picture of a stratum radiatum astrocyte patched with a pipette containing both dextran tetramethylrhodamine, a gap junction-impermeant dye used to localize the recorded cell (red, 0.1%), and 2-NBDG (green, 0.2%), diffusing to neighbouring gap junctional-coupled astrocytes. Scale bar, 20 μ m. Inset, whole-cell current profile from a CA1 astrocyte evoked by 150 ms voltage steps in 20 mV increments (-200 to $+40$ mV); scale bar, 1.5 nA, 15 ms. B, scheme of the hippocampus illustrating the arrangement of the stimulating electrode, CA1, CA3, and subiculum (SC).

~20 pA inward current in astrocytes, the EPSC paired pulse ratio was 1.91 ± 0.09 ($n = 5$).

These data show that although considerably smaller than neuronal responses, the synaptically evoked astroglial current is a reliable sensor of both moderate and strong neuronal activity.

Neuronal activity evokes a tripartite response in hippocampal astrocytes

To identify the nature of the evoked total astroglial current (I_{tot}), we dissected pharmacologically and molecularly the synaptically induced currents in astrocytes recorded concurrently with neuronal responses (fEPSPs; Fig. 2A). The majority of the slow inward current was due to potassium entry through $K_{\text{ir}}4.1$ channels (I_{K} , peak amplitude: -29 ± 6 pA, time of peak: 919 ± 424 ms, $n = 8$, Fig. 2A, B), as it was: (1) abolished by inhibition of postsynaptic glutamatergic activity by kynurenic acid (Fig. 2A), which represents the main source (80%) of neuronal potassium release (Poolos *et al.* 1987); (2) strongly reduced by barium, a potassium channel blocker (Fig. 3B; De Saint Jan & Westbrook, 2005; Djukic *et al.* 2007; Meeks & Mennerick, 2007; Bernardinelli & Chatton, 2008); and (3) absent in a conditional knockout mouse of the $K_{\text{ir}}4.1$ potassium channel subunit directed to astrocytes (GFAP-Cre- $K_{\text{ir}}4.1\text{fl/fl}$ mice, $K_{\text{ir}}4.1^{-/-}$; Fig. 2C), where basal evoked neuronal activity is unchanged (Djukic *et al.* 2007). Furthermore, the slow inward current displayed kinetics similar to the associated astroglial membrane potential depolarization (Fig. 1C, D), which is well known to reflect, with a quasi-nerstian relationship, changes in extracellular potassium (K^+) levels due to neuronal activity (Amzica, 2002; Amzica & Massimini, 2002; Amzica *et al.* 2002). The potassium conductance (I_{K}) represented the main component of the astroglial current, as it contributed to ~80% of the total astroglial charge transfer (I_{tot} : -120.5 ± 14 nA.ms, $n = 8$; I_{K} : -94.1 ± 16.2 nA.ms, $n = 8$; Fig. 2B).

The transient astroglial inward current persisting after inhibition of ionotropic GABA_A and GluRs (I_{GluT} , peak amplitude: -16.4 ± 3.4 pA; charge: -0.24 ± 0.06 nA.ms; time of peak: 8.9 ± 0.4 ms, $n = 8$) was due to the electrogenic uptake of glutamate, since it was abolished by TBOA, a broad-spectrum antagonist of GLT (Fig. 2A, B), as previously described (Bergles & Jahr, 1997; Diamond *et al.* 1998; Luscher *et al.* 1998; Pannasch *et al.* 2011). Due to its transient nature, I_{GluT} contributed to only ~0.2% of the total astroglial charge transfer (I_{tot} : -120.5 ± 14 nA.ms, $n = 8$; I_{GluT} : -0.24 ± 0.06 nA.ms, $n = 8$; Fig. 2B).

Finally, a small long-lasting residual current (I_{res}) persisted in the presence of picrotoxin, kynurenic acid and TBOA (I_{res} , peak amplitude: -9 ± 1.6 pA, time of peak: 232 ± 114 ms, $n = 8$; Fig. 2A, B). I_{res} was partially mediated (~40%) by electrogenic uptake of GABA, as it was decreased by nipecotic acid (1 mM), a competitive antagonist of GATs (GAT1/2/3 subtypes; Fig. 2D), which are expressed by astrocytes (Borden, 1996; Schousboe, 2000). The partial inhibition of I_{res} by nipecotic acid was not due to an extracellular build up of GABA, decreasing neuronal activity through activation of GABA receptors, because the effect of nipecotic acid persisted in the presence of GABA_A and GABA_B receptor blockers (picrotoxin and CGP55845, respectively) (I_{res} charge decrease: $-36 \pm 5\%$ $n = 5$ and $-41 \pm 7\%$ $n = 5$, in the absence and presence of picrotoxin (100 μM) and CGP55845 (2 μM), respectively). I_{res} was also partially mediated (~40%) by potassium entry, as it was inhibited by blockers of potassium channels such as quinine (200 μM) and tertiapin Q (100 nM) (Fig. 2D). However, I_{res} was neither mediated by a second messenger signalling via a G protein coupled receptor, as recently reported in Bergmann glial cells (Bellamy & Ogden, 2005), nor by astroglial calcium signalling. Indeed, I_{res} was insensitive to inhibitors of G proteins (GDP- β -S, 5 mM, intracellular delivery through the patch pipette), metabotropic glutamate and GABA_B receptors (LY341495, 20 μM ; CGP55845, 2 μM , respectively), as well as to intracellular calcium chelation (BAPTA, 10 mM)

to activate the SCs, the patch pipette electrode (grey), to record astrocytic currents, and the neuronal recording electrode (extracellular or patch pipette) (black), to record either fEPSPs or EPSCs, EPSPs and action potentials (APs), evoked by SC stimulation in the hippocampal CA1 area. C, sample traces of an inward current (I_{m} , black), recorded in voltage-clamp, and the concomitant membrane depolarization (V_{m} , grey), recorded in current-clamp, evoked in the same astrocyte by SC stimulation. Scale bar, 2.5 mV and 10 pA, 1 s. D, amplitude and kinetics of both signals (I_{m} and V_{m} ; $n = 6$). E, representative traces of simultaneous recordings of synaptically evoked currents in astrocytes (upper panel, grey) and neuronal fEPSPs (lower panel, black). Scale bar, 20 pA for astroglial current and 0.2 mV for fEPSPs, 25 ms. F, input–output curve illustrating the relationship between evoked presynaptic fibre volleys (input) and astroglial currents (output), recorded simultaneously ($n = 6$). G and I, representative traces of simultaneous recordings of synaptically evoked currents in astrocytes (left traces, grey) and evoked EPSCs (G) or EPSPs and APs (I) in single pyramidal neurons (right traces, black). Scale bars, 60 pA for astroglial current and 100 pA for EPSCs, 50 ms (G) and 60 pA for astroglial current and 20 mV for EPSPs and APs, 100 ms (I). H and J, the relationship between evoked astroglial currents and neuronal EPSCs (H) or APs (J), recorded simultaneously in dual whole cell recordings ($n = 5$).

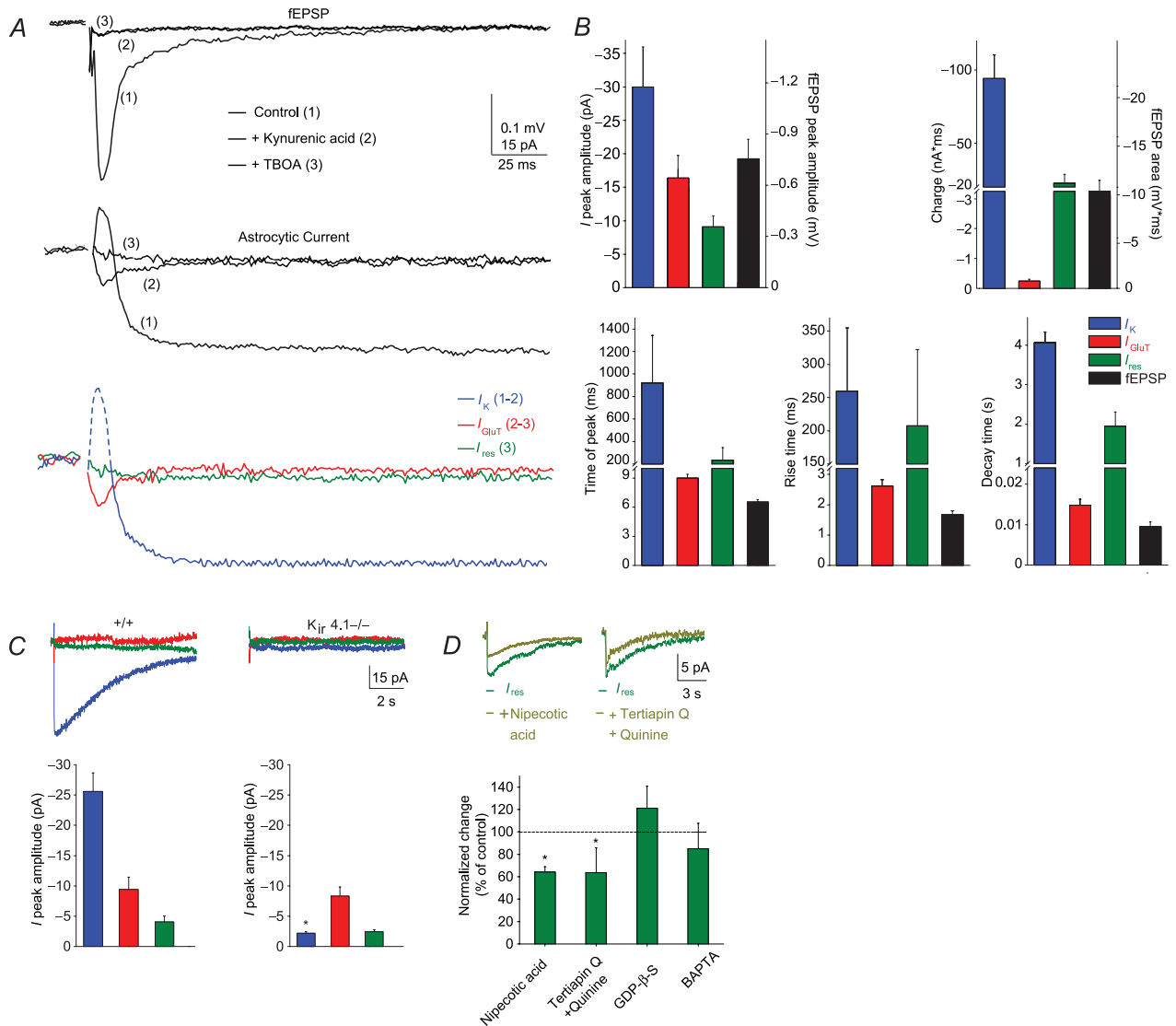


Figure 2. Identification of the synaptically evoked astroglial currents

A, sample traces of simultaneously recorded neuronal response (fEPSP, upper panel) and astroglial whole-cell currents (middle panel) induced by single stimulation of SCs in control conditions (picrotoxin, $100 \mu\text{M}$) (1, black trace), in the presence of kynurenic acid (ionotropic GluR antagonist, 5 mM) (2, dark grey trace) and subsequent application of TBOA (GLT antagonist, $200 \mu\text{M}$) (3, light grey trace). Sample traces of the pharmacologically isolated astroglial whole cell currents (I_K , I_{GluT} and I_{res}). Astrocytic I_K (blue) was isolated by subtracting the kynurenic acid-insensitive component (2) from the total current (1). Note that the initial fast outward current component (dash blue line) reflects fEPSP generated by adjacent pyramidal cells, while I_K corresponds to the slow inward current (solid blue line). The kynurenic acid-insensitive component current (2) consists of a fast inward current and a slow residual component of smaller amplitude (I_{res}), which was isolated by subsequent application of TBOA (3, green). Subtraction of I_{res} from the response in kynurenic acid isolates the GLT current (I_{GluT} , 2 and 3, red). Scale bar, 0.1 mV for fEPSP, 15 pA for astroglial current, 25 ms . B, comparison of the strength and dynamics of the astroglial current components and neuronal responses. C, sample traces and quantification of the three pharmacologically isolated astroglial current components (I_K , I_{GluT} and I_{res}) in wild type ($n = 5$) and $K_{ir4.1}$ glial conditional knockout mice ($K_{ir4.1-/-}$; $n = 5$). Note that I_{GluT} and I_{res} are similar in both genotypes, while I_K is fully abolished in $K_{ir4.1-/-}$ mice. Scale bar, 5 pA , 2 s . D, identification of the slow residual current (I_{res}) components. Quantification of I_{res} in the presence of several pharmacological treatments (nipecotic acid, GABA transporter inhibitor, 1 mM , $n = 5$; tertipatin Q, K_{ir} channel blocker, 100 nM ; and quinine, K_{ir} and K_{2P} channel blocker, $200 \mu\text{M}$, $n = 5$; intracellular GDP- β -S, 5 mM , $n = 6$; intracellular BAPTA, 10 mM , $n = 5$), revealing that astroglial I_{res} is partially mediated by GABA transporter and potassium inward currents. Scale bar, 20 pA , 3 s . Asterisks indicate statistically significant differences ($P < 0.05$).

(I_{res} charge, % of control: GDP- β -S: $120 \pm 20\%$, $n = 6$; LY341495: $105 \pm 12\%$, $n = 10$; CGP55845: $105 \pm 26\%$, $n = 6$; BAPTA: $93 \pm 36\%$, $n = 5$; Figs 2D and 3B). Although small in amplitude, I_{res} contributed to $\sim 20\%$ of the total astroglial charge, due to its slow kinetics (I_{tot} : -120.5 ± 14 nA.ms, $n = 8$; I_{res} : -22.5 ± 6 nA.ms, $n = 8$, Fig. 2B).

Thus, there are two temporally distinct types of synaptically evoked currents in hippocampal astrocytes: the fast inward I_{GluT} , which has similar kinetics to the neuronal response (I_{GluT} , rise time: 2.6 ± 0.2 ms; decay time: 14.8 ± 1.4 ms; fEPSP, rise time: 1.7 ± 0.1 ms, decay time: 9.5 ± 1.2 ms, $n = 8$); and the long-lasting (>10 s) inward currents, whose kinetics are slower than that of neuronal response by three orders of magnitudes (I_K , rise time: 259 ± 95 ms, decay time: 4059 ± 277 ms, $n = 8$; I_{res} rise time: 207 ± 114 ms, decay time: 1949 ± 358 ms, $n = 8$; Fig. 2B).

Differential activity dependence of the astrocytic evoked currents

The synaptically evoked astroglial inward currents were activity-dependent, as they were abolished when action potentials were inhibited by tetrodotoxin (TTX, $0.5 \mu\text{M}$, $n = 5$; Fig. 3A, B), as previously shown (Bergles & Jahr, 1997). This also demonstrates that these currents were not activated by direct electrical stimulation of astrocytes. Interestingly, the total current (I_{tot}) evoked in astroglia was, in contrast to the residual current (I_{res}), partially

dependent on synaptic activity mediated by NMDA receptors (NMDAR) ($\sim -40\%$ in CPP, an NMDAR antagonist, $10 \mu\text{M}$; Fig. 3B). This suggests that astroglial currents were induced by moderate to strong levels of neuronal activation. In contrast, metabotropic glutamate and GABA_B receptors do not regulate the total and residual astroglial currents (Fig. 3B). Finally, the activity dependence of the three astroglial currents we identified (I_K , I_{GluT} and I_{res}) is also demonstrated by the increase in their amplitude with the stimulation intensity, recruiting additional fibres. Indeed, as performed for the total astroglial current (Fig. 1F), we evaluated the strength of neuron to glia transmission for each astroglial current, by comparing their amplitudes (output) to those of the presynaptic fibre volley (input) for various stimulation intensities, using synchronous recordings of neuronal and astroglial responses (Fig. 4). We found that astrocytic I_{GluT} increased linearly with the neuronal input (Fig. 4C, D), similarly to the postsynaptic response, which was monitored by fEPSP (Fig. 4A, B). However, astroglial I_K and I_{res} behaved differently from the neuronal responses. I_K was strongly potentiated for moderate stimulations, although less so for higher amplitude stimulations (Fig. 4C, D). In contrast, the sensitivity of the residual current to the increase in recruited fibres was lower over a wide range of stimulation intensities compared to astroglial I_K and I_{GluT} (Fig. 4C, D).

Thus, these data show that I_K , I_{GluT} and I_{res} monitor differentially synaptic activity, and suggest that of the three astroglial currents, I_{GluT} is the most reliable sensor of excitatory synaptic activity.

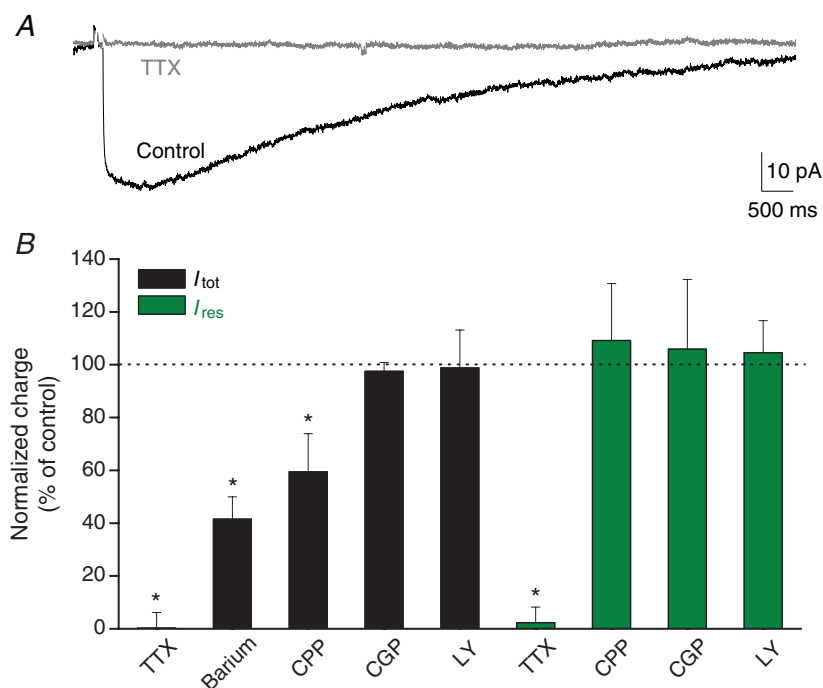


Figure 3. Activity dependence of astroglial evoked currents

A, sample traces of the total current evoked in astrocytes (I_{tot}) after SC stimulation before (black) and after (grey) application of TTX ($0.5 \mu\text{M}$). Scale bar, 10 pA, 500 ms. B, bar graph quantifying the effect of several pharmacological treatments on the total and the pharmacologically isolated residual currents evoked synaptically in astrocytes (TTX, $0.5 \mu\text{M}$, $n = 5$ for I_{tot} and $n = 5$ for I_{res} ; barium (potassium channel blocker, $200 \mu\text{M}$), $n = 5$; CPP (NMDAR antagonist, $10 \mu\text{M}$), $n = 6$ for I_{tot} and $n = 5$ for I_{res} ; CGP55845 (GABA_B receptor antagonist, CGP, $2 \mu\text{M}$), $n = 5$ for I_{tot} and $n = 6$ for I_{res} ; LY341495 (metabotropic GluR antagonist, LY, $20 \mu\text{M}$), $n = 5$ for I_{tot} and $n = 10$ for I_{res}). Note that both I_{tot} and I_{res} are dependent on AP firing, while only I_{tot} is partially induced by NMDAR activity. Asterisks indicate statistically significant differences ($P < 0.05$).

Alteration of synaptically evoked currents in disconnected astrocytes

A key property of astrocytes is the expression of high levels of gap junction channels, which mediate extensive direct inter-astroglial communication, and contribute to the network redistribution of many uptaken substances, such as potassium and glutamate (Pannasch & Rouach, 2013). We previously reported in a model of disconnected astrocytes (Cx30^{-/-}Cx43^{-/-} mice), in which gap junctional communication is totally disrupted (Wallraff *et al.* 2006; Pannasch *et al.* 2011), that astroglial I_K and I_{GluT} peak amplitudes are increased due to enhanced excitatory synaptic activity, and that astroglial potassium and glutamate clearance rates are decreased (Pannasch *et al.* 2011). Here we investigated whether the residual current (I_{res}) is also shaped by gap junctional communication in astrocytes. Dual recordings of astroglial slow residual currents and

synaptic responses (fEPSPs) revealed that I_{res} peak amplitude as well as I_{res} normalized peak amplitude to the simultaneously recorded excitatory transmission, calculated by the fEPSP slope/fibre volley ratio, were not significantly altered in Cx30^{-/-}Cx43^{-/-} astrocytes ($n = 8$; wild type, $n = 8$, Fig. S2A–C). However, we found that I_{res} exhibited slower decay kinetics in Cx30^{-/-}Cx43^{-/-} astrocytes (Cx30^{-/-}Cx43^{-/-}, 3.7 ± 0.5 s, $n = 8$; wild type, 2.4 ± 0.3 s, $n = 8$, Fig. S2D), as previously reported for I_K and I_{GluT} (Pannasch *et al.* 2011), suggesting that disconnected astrocytes inadequately uptake synaptically released potassium, glutamate and GABA.

The synaptically evoked currents in astrocytes exhibit differential short-term plasticity

Hippocampal excitatory synapses between SCs and CA1 pyramidal cells display several forms of short-term

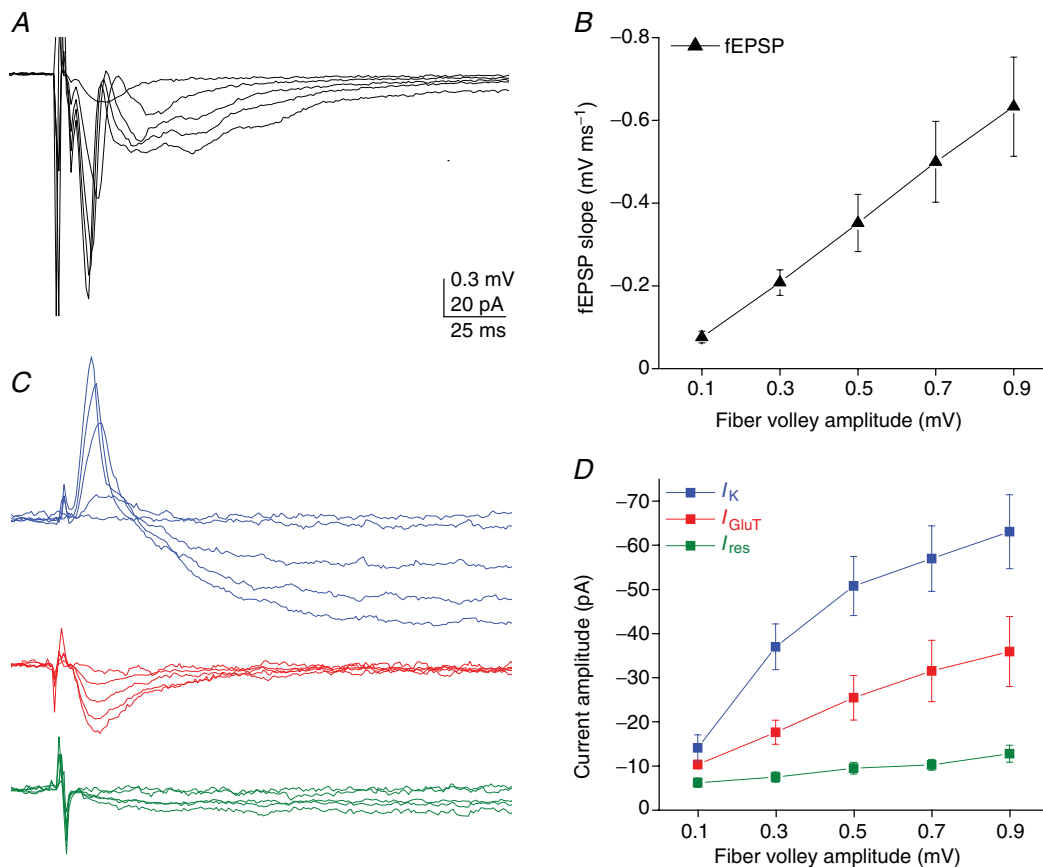


Figure 4. Activity dependence of dual synaptically evoked neuronal and astroglial responses

Simultaneous recordings of astrocytic and neuronal responses during SC stimulation (whole-cell and fEPSPs, respectively). A and C, representative traces of fEPSPs (A) and astroglial currents (I_K , I_{GluT} , I_{res}) (C) for different fiber volley amplitudes (0.1, 0.3, 0.5, 0.7 and 0.9 mV). Scale bar, 0.3 mV for fEPSPs, 20 pA for astroglial currents, 25 ms. B and D, input–output curves for fEPSPs (B) and the three astroglial currents (output) (D), illustrating their relationship to the evoked presynaptic fibre volleys (input) ($n = 5$). Note that all astroglial currents are sensitive to neuronal activity, with a linear increase in response to activity for I_{GluT} , a massive facilitation for I_K and only minimal sensitivity for I_{res} .

plasticity, such as paired-pulse facilitation, facilitating and depressing responses to prolonged repetitive stimulation, and post-tetanic potentiation (PTP), which all reflect changes in presynaptic release of glutamate. Because synaptically evoked currents in astrocytes are activity dependent, we investigated whether they also display the various forms of short-term plasticity typical of glutamatergic synaptic currents from CA1 pyramidal cells. To do so, we performed simultaneous recordings of neuronal fEPSPs and astroglial currents (I_{tot} , I_{K} , I_{GluT} and I_{res} in the same cell) in response to: (1) paired-pulse stimulation at different frequencies (0.5–50 Hz), (2) prolonged repetitive stimulation (10 Hz, 30 s) and (3) tetanic stimulation (100 Hz, 1 s) of SCs.

Classically, quantification of fast responses evoked repetitively in neurons involves measuring peak amplitudes in reference to pre-stimuli baselines, taken just before each stimulation. However, for slow evoked

responses such as astroglial I_{tot} , I_{K} and I_{res} , this type of quantification does not reflect the summation of astroglial currents over time, as they do not reach their peak amplitude and return to baseline before the start of the next stimulation, especially for short inter-stimulus intervals (< 10 s, Fig. S1). We thus analysed astroglial currents evoked repetitively by quantifying peak amplitudes with reference to the initial resting baseline (I_{res}), taken before the first stimulation (Fig. S1, and Methods).

We found that all astroglial currents (I_{tot} , I_{K} , I_{GluT} and I_{res}) displayed paired-pulse summation. However, only astroglial I_{GluT} exhibited a neuronal-like plasticity with similar amplitude and dynamics, i.e. a peak summation of ~ 1.5 fold at 25 Hz (paired-pulse summation at 20, 40 and 100 ms inter-stimulus interval: I_{GluT} : 1.38 ± 0.1 , 1.50 ± 0.17 , 1.39 ± 0.15 , $n = 5$; fEPSP: 1.26 ± 0.09 , 1.55 ± 0.2 , 1.36 ± 0.08 , $n = 5$; Fig. 5A, B). In contrast, the summation of I_{tot} , I_{K} and I_{res} occurred over a wide

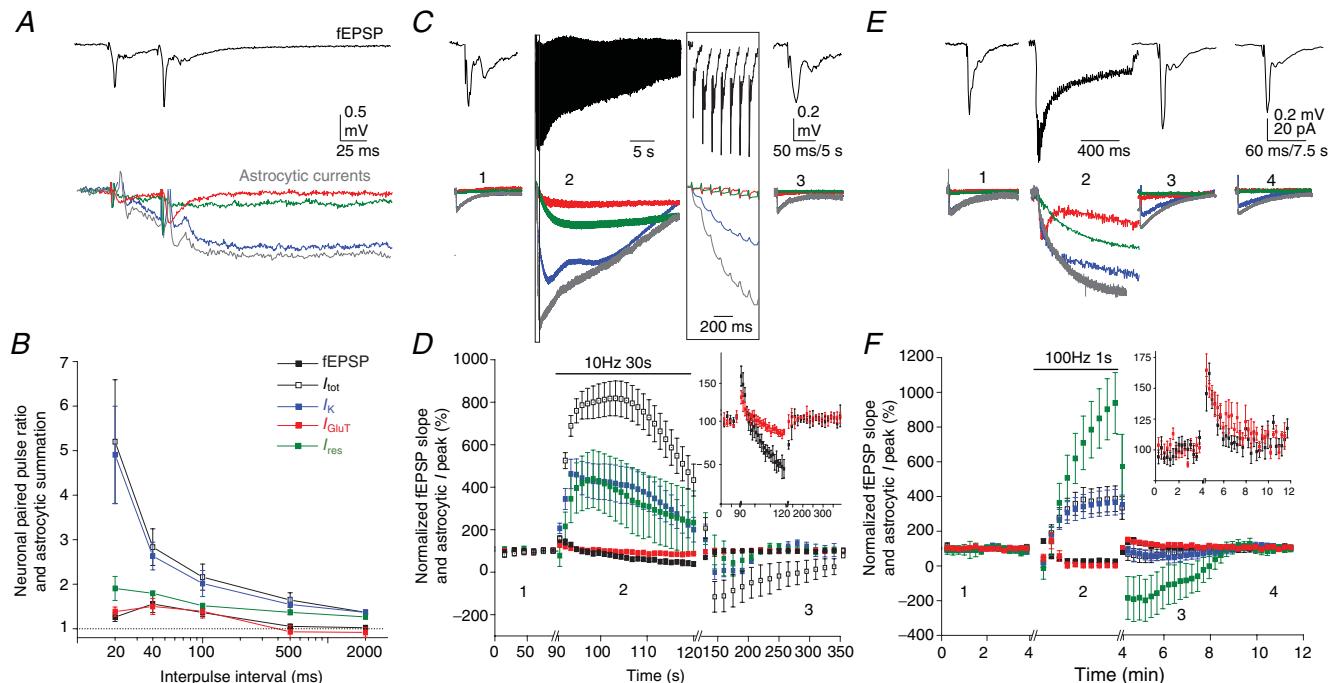


Figure 5. Differential short-term plasticity patterns of synaptically evoked astroglial currents compared to neuronal responses

Simultaneous recordings of synaptically evoked astroglial currents and fEPSPs in response to paired-pulse, repetitive and tetanic stimulation. **A** and **B**, paired-pulse facilitation of neuronal responses (fEPSPs) and summation of astroglial currents (I_{tot} , I_{K} , I_{GluT} and I_{res}). Sample traces are shown for paired-pulse stimulation at a 40 ms inter-pulse interval (**A**). Scale bar, 0.5 mV for fEPSPs, 20 pA for astroglial currents, 25 ms. **B**, quantification of paired-pulse ratios at different inter-pulse intervals ($n = 5$). **C** and **D**, responses to repetitive stimulation. Sample traces of fEPSPs and astroglial currents before (1), during (2) and after (3) prolonged repetitive stimulation (10 Hz, 30 s), as indicated (**C**). Scale bar, 0.2 mV for fEPSPs, 40 pA for astroglial currents, 5 s for astroglial currents and 50 ms for fEPSPs in (1) and (3), and 2 s in (2). **D**, fEPSP slopes and astroglial current peak amplitudes normalized to responses before the onset of stimulation (1) ($n = 5$); inset: zoom of fEPSP and astroglial I_{GluT} responses. **E** and **F**, responses to post-tetanic stimulation. **E**, sample traces of fEPSP and astroglial currents, as indicated on the graph, before (1), during (2) and after (3, 4) a single tetanic stimulation (100 Hz, 1 s) in the presence of 10 μM CPP (NMDAR antagonist). Scale bar, 0.2 mV for fEPSPs, 20 pA for astroglial currents, 7.5 s for astroglial currents and 60 ms for fEPSP in (1) (3) and (4), and 300 ms in (2). **F**, fEPSP slopes and astroglial current peak amplitudes normalized to responses before the onset of stimulation (1) ($n = 5$); inset: zoom of fEPSP and astroglial I_{GluT} responses.

range of interpulse intervals (from 20 ms to 2 s), and increased with the frequency of stimulation. Indeed, while I_{tot} and I_{K} had strong paired-pulse summation of ~ 5 at 50 Hz (I_{tot} : 5.20 ± 1.39 ; I_{K} : 4.95 ± 1 ; $n = 5$) compared to ~ 1.4 at 0.5 Hz (I_{tot} : 1.38 ± 0.04 ; I_{K} : 1.36 ± 0.03 ; $n = 5$), I_{res} had weaker paired-pulse summation of ~ 2 at 50 Hz (1.9 ± 0.1 , $n = 5$), comparable to synaptic paired-pulse facilitation, and ~ 1.3 at 0.5 Hz (1.26 ± 0.04 , $n = 5$) (Fig. 5A, B).

Similarly, we found a differential behaviour of astroglial I_{GluT} compared to I_{tot} , I_{K} and I_{res} in response to prolonged repetitive or tetanic stimulation (10 Hz, 30 s or 100 Hz, 1 s, respectively).

Repetitive stimulation of SCs results in an initial facilitation of excitatory synaptic transmission, due to the massive release of glutamate, followed by a subsequent depression, caused by the depletion of glutamate vesicular pools (Fig. 5C, D). Astroglial I_{GluT} , like fEPSPs, first potentiated and then depressed with a similar time course to that of neuronal responses, although with reduced magnitudes (Fig. 5D). In contrast, I_{tot} , I_{K} and I_{res} exhibited strong temporal summation ($\sim 800\%$ of baseline response for I_{tot} and $\sim 400\%$ for I_{K} and I_{res} , $n = 5$) compared to fEPSP potentiation ($\sim 150\%$ of baseline response, $n = 5$; Fig. 5D). In addition, the temporal summation of slow astroglial currents lasted longer than the potentiation of neuronal responses. Indeed, I_{tot} , I_{K} and I_{res} amplitudes reached peak values within ~ 3 – 12 s of 10 Hz stimulation, and then slowly decayed to half peak responses after 30 s, while fEPSPs reached their peak response within ~ 1 s and fully decayed to baseline level after ~ 5 s (Fig. 5D). Although astroglial I_{tot} was partially dependent on NMDAR activation in basal conditions (Fig. 3B), the responses of astroglial current components (I_{K} , I_{GluT} and I_{res}) to repetitive stimulation did not involve the activity of NMDARs (data not shown).

Tetanic stimulation of SCs (100 Hz, 1 s) results in PTP, a transient potentiation lasting a few minutes. During the tetanus, astroglial I_{GluT} initially potentiated and then depressed, as neuronal responses (Fig. 5E, F). In contrast, I_{tot} , I_{K} and I_{res} displayed marked summation, as during repetitive stimulation. Interestingly, I_{res} exhibited the highest summation during tetanic stimulation ($\sim 900\%$ of baseline response vs. $\sim 370\%$ for I_{tot} and I_{K} , $n = 6$; Fig. 5F). The normalized summation of astroglial I_{tot} , I_{K} and I_{res} actually reflected the depolarization of astrocytes induced by prolonged repetitive stimulation (ΔV_{m} for I_{tot} : 15.3 ± 2.8 mV; I_{K} : 10.4 ± 2.4 mV; and I_{res} : 5.3 ± 2.2 mV, $n = 5$) or by tetanic stimulation (ΔV_{m} for I_{tot} : 6.5 ± 0.9 mV; I_{K} : 6.2 ± 1.1 mV; and I_{res} : 5.2 ± 1.5 mV, $n = 6$). Finally, after the tetanus, only I_{GluT} displayed a PTP of $\sim 65\%$ ($64 \pm 13\%$, $n = 6$), as neurons ($67 \pm 7\%$, $n = 6$) with a similar time course, while I_{tot} , I_{K} and I_{res} exhibited a post-tetanic depression, with a peak depression at 1 min after the tetanus of $\sim -60\%$ for I_{tot} , -70% for I_{K} and

$\sim -400\%$ for I_{res} ($n = 6$), slowly coming back to baseline 5 min after the tetanus (Fig. 5F).

Together, these data show that while I_{GluT} remarkably monitors short-term excitatory synaptic plasticity, I_{K} and I_{res} display differential plasticity patterns compared to neighbouring synapses.

Astroglial potassium clearance through $K_{\text{ir}}4.1$ channels contributes to hippocampal short-term synaptic plasticity

The slow potassium current contributes to 80% of the synaptically evoked total current identified in hippocampal astrocytes (Fig. 2A, B), is mediated by $K_{\text{ir}}4.1$ channels (Fig. 2C) and is activity dependent (Fig. 4C, D), displaying short-term plasticity (Fig. 5). We thus investigated whether potassium clearance through $K_{\text{ir}}4.1$ channels regulates some forms of hippocampal CA1 short-term synaptic plasticity that involve strong neuronal release of potassium. To do so, we used the glial conditional $K_{\text{ir}}4.1$ knockout mice ($K_{\text{ir}}4.1$ fl/fl:hGFAP-Cre mice, $K_{\text{ir}}4.1^{-/-}$) and examined neuronal responses to prolonged repetitive and tetanic stimulation of SCs. We found that responses to prolonged repetitive stimulation (10 Hz, 30 s) initially facilitated more (normalized fEPSP slope of the first response during repetitive stimulation, +/+, $146 \pm 6\%$ $n = 6$; $K_{\text{ir}}4.1^{-/-}$, $204 \pm 9\%$ $n = 9$, $P < 0.001$) in $K_{\text{ir}}4.1^{-/-}$ mice, while subsequent depression and recovery to baseline responses were similar in wild-type and $K_{\text{ir}}4.1^{-/-}$ mice (+/+, $95 \pm 11\%$ $n = 6$; $K_{\text{ir}}4.1^{-/-}$, $103 \pm 13\%$ $n = 9$, Fig. 6A). This suggests an initial increase in glutamate release in $K_{\text{ir}}4.1^{-/-}$ mice, followed by a similar vesicle pool depression and replenishment during the 10 Hz train in both mice. Furthermore, in response to tetanic stimulation (100 Hz, 1 s), $K_{\text{ir}}4.1^{-/-}$ mice had a stronger PTP than wild-type mice. Indeed, up to 5 min after the stimulation, responses potentiated by $\sim +80\%$ in $K_{\text{ir}}4.1^{-/-}$ mice (normalized fEPSP slope measured directly after tetanization, +/+, $164 \pm 7\%$, $n = 6$; $K_{\text{ir}}4.1^{-/-}$, $221 \pm 18\%$, $n = 8$, $P \leq 0.05$; Fig. 6B) and decayed back to baseline more slowly compared to wild-type mice (normalized fEPSP slope measured 3 min after the tetanus, +/+, $109 \pm 6\%$, $n = 6$; $K_{\text{ir}}4.1^{-/-}$, $165 \pm 22\%$, $n = 8$, $P \leq 0.05$; Fig. 6B). This suggests that during the tetanus, more glutamate is released to induce PTP in $K_{\text{ir}}4.1^{-/-}$ mice.

Discussion

We demonstrate here that hippocampal astrocytes display several activity-dependent currents which have, except for I_{GluT} currents, differential short-term plasticity patterns compared to surrounding synapses. We also show that, in turn, the main synaptically evoked currents in astrocytes,

mediated by potassium entry through $K_{ir}4.1$ channels, alter hippocampal short-term synaptic plasticity. These results provide important novel insights into the dynamics and plasticity of neuroglial interactions involving ionic channels and regulating synaptic plasticity.

Two types of synaptically evoked currents in hippocampal astrocytes

Hippocampal astrocytes display several currents induced by single stimulation of SCs, with two main temporal dynamics: a transient GLT current, a long-lasting potassium current mediated by $K_{ir}4.1$ channels, and a previously reported, but yet unidentified, slow residual current (Bergles & Jahr, 1997; Clark & Barbour, 1997; Luscher *et al.* 1998). We found that the slow residual current (I_{res}) persists in hippocampal astrocytes after blockade of $K_{ir}4.1$ channels, glutamatergic receptors and GLTs, and is partially mediated by GATs and $K_{ir}4.1$ -independent potassium channels. Long-lasting GAT currents evoked synaptically have already been identified in astrocytes from other brain regions such as the neocortex (Kinney & Spain, 2002), and display slow rise and decay kinetics, in contrast to GLT currents. In addition, as previously suggested, part of I_{res} probably reflects potassium efflux by presynaptic elements generating action potentials (Bergles & Jahr, 1997), but is not mediated by $K_{ir}4.1$ channels. In particular, $K_{ir}5.1$, $K_{ir}2.1$, $K_{ir}2.2$, $K_{ir}2.3$ or two-pore-domain (K_{2P}) potassium channels, expressed in hippocampal astrocytes (Schroder

et al. 2002; Seifert *et al.* 2009; Zhou *et al.* 2009), probably mediate this residual potassium current, sensitive to K_{ir} and K_{2P} channel blockers.

What may account for the different kinetics of fast and slow currents in astrocytes? They probably reflect differences in extracellular concentrations of glutamate, potassium and GABA over time, originating from distinct release and clearance properties. Glutamate is mostly released by presynaptic elements at confined synaptic active zones. The close vicinity of glutamate release sites and clustered astroglial GLTs (Melone *et al.* 2009) probably enables efficient fast glutamate clearance. In contrast, the distal location of astroglial GATs to GABAergic synapses (Minelli *et al.* 1996) may underlie the slow kinetics of the synaptically evoked GAT currents. Finally, despite abundant expression of $K_{ir}4.1$ channels preferentially located on astrocytic processes enwrapping synapses (Higashi *et al.* 2001), the slow astroglial potassium clearance may originate from uniform extracellular potassium bulk rises, due to pre- and postsynaptic release of potassium (Poolos *et al.* 1987) over large zones, which may be slowly redistributed through gap junction-mediated networks (Wallraff *et al.* 2006; Pannasch *et al.* 2011).

Differential activity dependence and short-term plasticity of astroglial responses

We show that astroglial currents are activity dependent, and can sense reliably moderate to strong neuronal

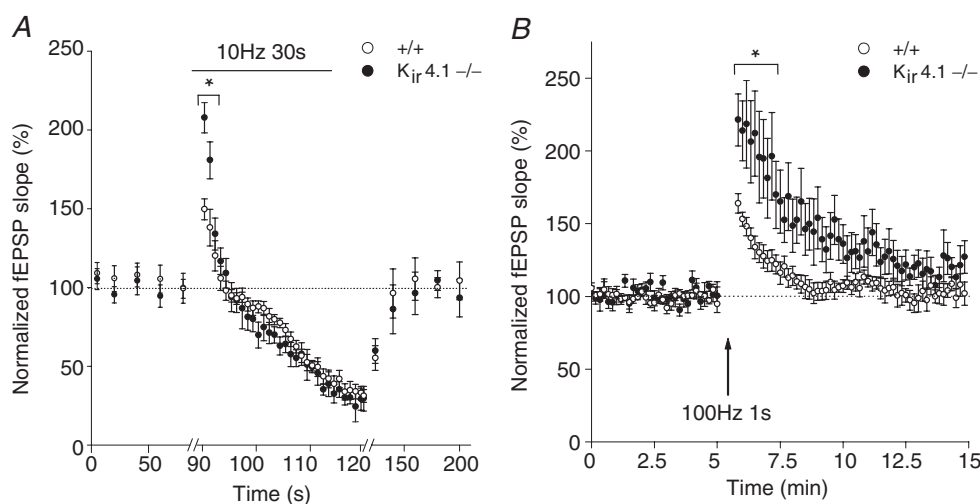


Figure 6. $K_{ir}4.1$ -mediated potassium uptake in astrocytes downregulates hippocampal short-term synaptic plasticity

Responses to prolonged repetitive stimulation (10 Hz, 30 s) (A) and post-tetanic potentiation induced by a single tetanus (100 Hz, 1 s), in the presence of CPP (NMDAR antagonist, 10 μ M) (B) are increased in glial conditional $K_{ir}4.1^{-/-}$ mice (closed circles, $n = 5$ and $n = 6$, respectively) compared to wild-type mice (open circles, $n = 5$). The tetanus is indicated by the arrow in B. Responses to repetitive stimulation and post-tetanic potentiation were normalized to fEPSP slopes measured before the onset of stimulation. Asterisks indicate statistically significant differences ($P < 0.05$).

activity. Astroglial currents of modest amplitudes (10–60 pA) are associated with stronger excitatory synaptic transmission (EPSCs 100–500 pA) and action potential firing, and depend partially on NMDAR activation. Interestingly, the astroglial current components have different sensitivity to neuronal activity evoked by single stimulation of SCs. Indeed, we found that in contrast to I_{GluT} , which is a reliable sensor of excitatory synaptic strength, as previously shown (Diamond *et al.* 1998; Luscher *et al.* 1998), I_{K} already strongly potentiates for moderate stimulation, while I_{res} displays the lowest sensitivity. The differential sensitivities of astroglial current components to neuronal activity probably explain why in $\text{Cx}30^{-/-}\text{Cx}43^{-/-}$ mice, in which astrocytes are disconnected and synaptic activity is enhanced, peak amplitudes of I_{K} and I_{GluT} are enhanced (Pannasch *et al.* 2011), while that of I_{res} is unchanged.

Similarly, astroglial currents display differential short-term plasticity patterns compared to neighbouring synapses, except for I_{GluT} , which exhibits a neuronal-like short-term plasticity in response to paired-pulse, prolonged repetitive and tetanic stimulation of SCs. I_{K} and I_{res} display an alternative short-term plasticity profile, with stronger summation for higher stimulation frequency during paired-pulse, resulting in a marked summation for I_{K} (~5-fold). I_{K} and I_{res} also exhibit strong and sustained summation over time during repetitive and tetanic stimulations, probably reflecting the astroglial integration of previous neuronal activity. In addition, I_{K} and I_{res} do not show PTP, but instead display a post-tetanic depression, resembling undershoot responses following high-frequency stimulations (D'Ambrosio *et al.* 2002). Such undershoot responses may serve to spatially redistribute released potassium in the extracellular space, as clearance of excess potassium needs to be transient to avoid depletion of neuronal potassium. The difference in short-term plasticity patterns between I_{GluT} and $I_{\text{K}}/I_{\text{res}}$ suggests that factors other than increased release probability, leading to summation of extracellular potassium levels, are probably involved in I_{K} and I_{res} summation during stimulation trains, as already suggested for AMPAR current facilitation in Bergmann glia (Bellamy & Ogden, 2005). The astroglial depolarizations that we detected during trains of stimulation support this hypothesis. In addition, the slow kinetics of I_{K} and I_{res} probably account for their strong temporal summation, as both currents are not fully inactivated in between stimulation frequencies >10 Hz. Altogether, we show that the strength of neuron-to-glia signalling in the hippocampus is dynamically regulated by the frequency of SC stimulation. Our data are in accordance with the few previous studies exploring short-term plasticity of glial currents, mostly paired-pulse facilitation, at various synapses (Matsui & Jahr, 2004; Bellamy & Ogden, 2005; Manita *et al.* 2007; Goubard *et al.* 2011).

Integration of synaptic *versus* non-synaptic signals might govern the pattern of astroglial short-term plasticity, and may be important for astrocytes to sense and sustain high-frequency synaptic activity.

Astroglial $\text{K}_{\text{ir}}4.1$ channels down-regulate short-term synaptic plasticity

We reveal that $\text{K}_{\text{ir}}4.1$ channels down-regulate two forms of short-term synaptic plasticity: responses to prolonged repetitive stimulation and PTP. The short-term dynamics of astrocytic potassium clearance that we identified during repetitive and tetanic stimulation (Fig. 5) might contribute to the associated hippocampal short-term synaptic plasticity. However, there is no experimental tool to directly test this hypothesis in a native context, because we cannot block specifically the astroglial short-term dynamics. Indeed, there is no selective glial blocker of $\text{K}_{\text{ir}}4.1$ -mediated potassium uptake that could be used in a dose-dependent manner. Both short-term synaptic plasticities, responses to prolonged repetitive stimulation and PTP, reflect changes in pre-synaptic glutamate release, suggesting that astroglial $\text{K}_{\text{ir}}4.1$ channels decrease glutamate release by pre-synaptic terminals. Such regulation of presynaptic release by $\text{K}_{\text{ir}}4.1$ channels during repetitive stimulation and PTP may be directly mediated by their control of extracellular potassium levels, which modulate neuronal excitability, release probability and synaptic efficacy in the hippocampus (Izquierdo *et al.* 1971; Hablitz & Lundervold, 1981; Balestrino *et al.* 1986; Poolos *et al.* 1987; Poolos & Kocsis, 1990; Raffaelli *et al.* 2004), although neuronal excitability was reported to be unchanged in $\text{K}_{\text{ir}}4.1^{-/-}$ mice (Djukic *et al.* 2007). Alternatively, indirect changes in gliotransmitter release, due to altered astroglial intracellular signalling mediated by the control of astroglial membrane potential by $\text{K}_{\text{ir}}4.1$ channels (Djukic *et al.* 2007; Chever *et al.* 2010), may also decrease presynaptic glutamate release by a variety of mechanisms. However, unlike previous studies (Djukic *et al.* 2007; Kucheryavykh *et al.* 2007), we did not find that $\text{K}_{\text{ir}}4.1^{-/-}$ mice had decreased astroglial glutamate transport, suggesting that astroglial $\text{K}_{\text{ir}}4.1$ -mediated potassium uptake directly impacts presynaptic glutamate release during short-term plasticity. The discrepancy with our study may arise from the fact that we induced GLT currents by single stimulation of SCs, resulting in moderate potassium release, insufficient in $\text{K}_{\text{ir}}4.1^{-/-}$ mice to alter significantly ion gradient-dependent GLT uptake. In contrast, GLT currents were evoked by stronger stimulations (50 Hz train with barium; Djukic *et al.* 2007), probably inducing stronger extracellular potassium accumulation in $\text{K}_{\text{ir}}4.1^{-/-}$ mice, and subsequent disruption of ion gradients necessary for proper

GLT uptake. In addition, glutamate uptake was indirectly assessed in Kucheryavykh *et al.* (2007), as only extracellular glutamate levels were measured after glutamate bulk loading in cultured astrocytes. Thus, the increased extracellular glutamate levels observed with $K_{ir4.1}^{-/-}$ astrocytes could solely result from enhanced glutamate release by depolarized astrocytes. Together with previous results showing enhanced hippocampal LTP in $K_{ir4.1}^{-/-}$ mice (Djukic *et al.* 2007), and inhibition of long-term depression maintenance by reduction of glial potassium uptake (Janigro *et al.* 1997), our data indicate that astrocytic $K_{ir4.1}$ -mediated potassium uptake is an important negative regulator of synaptic potentiation. It can be speculated that astrocytic potassium clearance restricts the potentiation to synapses specifically activated, by limiting potassium diffusion to adjacent dendrites. Thus, astrocytes, by regulating extracellular potassium levels, may define the signal-to-noise ratio important for specific strengthening of synaptic contacts and synchronization of neuronal populations, the prerequisite for learning and memory.

References

- Amzica F (2002). In vivo electrophysiological evidences for cortical neuron–glia interactions during slow (<1 Hz) and paroxysmal sleep oscillations. *J Physiol Paris* **96**, 209–219.
- Amzica F & Massimini M (2002). Glial and neuronal interactions during slow wave and paroxysmal activities in the neocortex. *Cereb Cortex* **12**, 1101–1113.
- Amzica F, Massimini M & Manfridi A (2002). Spatial buffering during slow and paroxysmal sleep oscillations in cortical networks of glial cells *in vivo*. *J Neurosci* **22**, 1042–1053.
- Balestrino M, Aitken PG & Somjen GG (1986). The effects of moderate changes of extracellular K^+ and Ca^{2+} on synaptic and neural function in the CA1 region of the hippocampal slice. *Brain Res* **377**, 229–239.
- Bellamy TC & Ogden D (2005). Short-term plasticity of Bergmann glial cell extrasynaptic currents during parallel fiber stimulation in rat cerebellum. *Glia* **52**, 325–335.
- Bellamy TC & Ogden D (2006). Long-term depression of neuron to glial signalling in rat cerebellar cortex. *Eur J Neurosci* **23**, 581–586.
- Ben Achour S & Pascual O (2012). Astrocyte–neuron communication: functional consequences. *Neurochem Res* **37**, 2464–2473.
- Bergles DE, Jabs R & Steinhauser C (2010). Neuron–glia synapses in the brain. *Brain Res Rev* **63**, 130–137.
- Bergles DE & Jahr CE (1997). Synaptic activation of glutamate transporters in hippocampal astrocytes. *Neuron* **19**, 1297–1308.
- Bernardinelli Y & Chatton JY (2008). Differential effects of glutamate transporter inhibitors on the global electrophysiological response of astrocytes to neuronal stimulation. *Brain Res* **1240**, 47–53.
- Borden LA (1996). GABA transporter heterogeneity: pharmacology and cellular localization. *Neurochem Int* **29**, 335–356.
- Chever O, Djukic B, McCarthy KD & Amzica F (2010). Implication of $K_{ir4.1}$ channel in excess potassium clearance: an *in vivo* study on anesthetized glial-conditional $K_{ir4.1}$ knock-out mice. *J Neurosci* **30**, 15769–15777.
- Clark BA & Barbour B (1997). Currents evoked in Bergmann glial cells by parallel fibre stimulation in rat cerebellar slices. *J Physiol* **502**, 335–350.
- D'Ambrosio R, Gordon DS & Winn HR (2002). Differential role of KIR channel and Na^+/K^+ -pump in the regulation of extracellular K^+ in rat hippocampus. *J Neurophysiol* **87**, 87–102.
- De Saint Jan D & Westbrook GL (2005). Detecting activity in olfactory bulb glomeruli with astrocyte recording. *J Neurosci* **25**, 2917–2924.
- Diamond JS, Bergles DE & Jahr CE (1998). Glutamate release monitored with astrocyte transporter currents during LTP. *Neuron* **21**, 425–433.
- Djukic B, Casper KB, Philpot BD, Chin LS & McCarthy KD (2007). Conditional knock-out of $K_{ir4.1}$ leads to glial membrane depolarization, inhibition of potassium and glutamate uptake, and enhanced short-term synaptic potentiation. *J Neurosci* **27**, 11354–11365.
- Drummond GB (2009). Reporting ethical matters in *The Journal of Physiology*: standards and advice. *J Physiol* **587**, 713–719.
- Filosa A, Paixao S, Honsek SD, Carmona MA, Becker L, Feddersen B, Gaitanos L, Rudhard Y, Schoepfer R, Klopstock T, Kullander K, Rose CR, Pasquale EB & Klein R (2009). Neuron–glia communication via EphA4/ephrin-A3 modulates LTP through glial glutamate transport. *Nat Neurosci* **12**, 1285–1292.
- Ge WP & Duan S (2007). Persistent enhancement of neuron–glia signaling mediated by increased extracellular K^+ accompanying long-term synaptic potentiation. *J Neurophysiol* **97**, 2564–2569.
- Genoud C, Quairiaux C, Steiner P, Hirling H, Welker E & Knott GW (2006). Plasticity of astrocytic coverage and glutamate transporter expression in adult mouse cortex. *PLoS Biol* **4**, e343.
- Goubard V, Fino E & Venance L (2011). Contribution of astrocytic glutamate and GABA uptake to corticostriatal information processing. *J Physiol* **589**, 2301–2319.
- Hablitz JJ & Lundervold A (1981). Hippocampal excitability and changes in extracellular potassium. *Exp Neurol* **71**, 410–420.
- Henneberger C, Papouin T, Oliet SH & Rusakov DA (2010). Long-term potentiation depends on release of D-serine from astrocytes. *Nature* **463**, 232–236.
- Henneberger C & Rusakov DA (2012). Monitoring local synaptic activity with astrocytic patch pipettes. *Nat Protoc* **7**, 2171–2179.
- Higashi K, Fujita A, Inanobe A, Tanemoto M, Doi K, Kubo T & Kurachi Y (2001). An inwardly rectifying K^+ channel, Kir4.1, expressed in astrocytes surrounds synapses and blood vessels in brain. *Am J Physiol Cell Physiol* **281**, C922–931.
- Huang YH, Sinha SR, Tanaka K, Rothstein JD & Bergles DE (2004). Astrocyte glutamate transporters regulate metabotropic glutamate receptor-mediated excitation of hippocampal interneurons. *J Neurosci* **24**, 4551–4559.

- Iino M, Goto K, Kakegawa W, Okado H, Sudo M, Ishiuchi S, Miwa A, Takayasu Y, Saito I, Tsuzuki K & Ozawa S (2001). Glia–synapse interaction through Ca^{2+} -permeable AMPA receptors in Bergmann glia. *Science* **292**, 926–929.
- Izquierdo I, Nasello AG & Marichich ES (1971). The dependence of hippocampal function on extracellular potassium levels. *Curr Mod Biol* **4**, 35–46.
- Janigro D, Gasparini S, D'Ambrosio R, McKhann G, 2nd & DiFrancesco D (1997). Reduction of K^+ uptake in glia prevents long-term depression maintenance and causes epileptiform activity. *J Neurosci* **17**, 2813–2824.
- Karwoski CJ, Coles JA, Lu HK & Huang B (1989). Current-evoked transcellular K^+ flux in frog retina. *J Neurophysiol* **61**, 939–952.
- Kinney GA & Spain WJ (2002). Synaptically evoked GABA transporter currents in neocortical glia. *J Neurophysiol* **88**, 2899–2908.
- Kucheryavykh YV, Kucheryavykh IY, Nichols CG, Maldonado HM, Baksi K, Reichenbach A, Skatchkov SN & Eaton MJ (2007). Downregulation of Kir4.1 inward rectifying potassium channel subunits by RNAi impairs potassium transfer and glutamate uptake by cultured cortical astrocytes. *Glia* **55**, 274–281.
- Luscher C, Malenka RC & Nicoll RA (1998). Monitoring glutamate release during LTP with glial transporter currents. *Neuron* **21**, 435–441.
- Manita S, Suzuki T, Inoue M, Kudo Y & Miyakawa H (2007). Paired-pulse ratio of synaptically induced transporter currents at hippocampal CA1 synapses is not related to release probability. *Brain Res* **1154**, 71–79.
- Matsui K & Jahr CE (2004). Differential control of synaptic and ectopic vesicular release of glutamate. *J Neurosci* **24**, 8932–8939.
- Matthias K, Kirchhoff F, Seifert G, Huttmann K, Matyash M, Kettenmann H & Steinhauser C (2003). Segregated expression of AMPA-type glutamate receptors and glutamate transporters defines distinct astrocyte populations in the mouse hippocampus. *J Neurosci* **23**, 1750–1758.
- Meeks JP & Mennerick S (2007). Astrocyte membrane responses and potassium accumulation during neuronal activity. *Hippocampus* **17**, 1100–1108.
- Melone M, Bellesi M & Conti F (2009). Synaptic localization of GLT-1a in the rat somatic sensory cortex. *Glia* **57**, 108–117.
- Minelli A, DeBiasi S, Brecha NC, Zuccarello LV & Conti F (1996). GAT-3, a high-affinity GABA plasma membrane transporter, is localized to astrocytic processes, and it is not confined to the vicinity of GABAergic synapses in the cerebral cortex. *J Neurosci* **16**, 6255–6264.
- Nedergaard M & Verkhratsky A (2012). Artifact versus reality – how astrocytes contribute to synaptic events. *Glia* **60**, 1013–1023.
- Oliet SH & Bonfardin VD (2010). Morphological plasticity of the rat supraoptic nucleus – cellular consequences. *Eur J Neurosci* **32**, 1989–1994.
- Oliet SH, Piet R & Poulain DA (2001). Control of glutamate clearance and synaptic efficacy by glial coverage of neurons. *Science* **292**, 923–926.
- Omrani A, Melone M, Bellesi M, Safiulina V, Aida T, Tanaka K, Cherubini E & Conti F (2009). Up-regulation of GLT-1 severely impairs LTD at mossy fibre–CA3 synapses. *J Physiol* **587**, 4575–4588.
- Orkand RK, Nicholls JG & Kuffler SW (1966). Effect of nerve impulses on the membrane potential of glial cells in the central nervous system of amphibia. *J Neurophysiol* **29**, 788–806.
- Pannasch U & Rouach N (2013). Emerging role for astroglial networks in information processing: from synapse to behavior. *Trends Neurosci* **36**, 405–417.
- Pannasch U, Vargova L, Reingruber J, Ezan P, Holcman D, Giaume C, Sykova E & Rouach N (2011). Astroglial networks scale synaptic activity and plasticity. *Proc Natl Acad Sci U S A* **108**, 8467–8472.
- Piet R, Vargova L, Sykova E, Poulain DA & Oliet SH (2004). Physiological contribution of the astrocytic environment of neurons to intersynaptic crosstalk. *Proc Natl Acad Sci U S A* **101**, 2151–2155.
- Poolos NP & Kocsis JD (1990). Elevated extracellular potassium concentration enhances synaptic activation of *N*-methyl-D-aspartate receptors in hippocampus. *Brain Res* **508**, 7–12.
- Poolos NP, Mauk MD & Kocsis JD (1987). Activity-evoked increases in extracellular potassium modulate presynaptic excitability in the CA1 region of the hippocampus. *J Neurophysiol* **58**, 404–416.
- Raffaelli G, Saviane C, Mohajerani MH, Pedarzani P & Cherubini E (2004). BK potassium channels control transmitter release at CA3–CA3 synapses in the rat hippocampus. *J Physiol* **557**, 147–157.
- Rothstein JD, Dykes-Hoberg M, Pardo CA, Bristol LA, Jin L, Kuncl RW, Kanai Y, Hediger MA, Wang Y, Schielke JP & Welty DF (1996). Knockout of glutamate transporters reveals a major role for astroglial transport in excitotoxicity and clearance of glutamate. *Neuron* **16**, 675–686.
- Saab AS, Neumeyer A, Jahn HM, Cupido A, Simek AA, Boele HJ, Scheller A, Le Meur K, Gotz M, Monyer H, Sprengel R, Rubio ME, Deitmer JW, De Zeeuw CI & Kirchhoff F (2012). Bergmann glial AMPA receptors are required for fine motor coordination. *Science* **337**, 749–753.
- Schousboe A (2000). Pharmacological and functional characterization of astrocytic GABA transport: a short review. *Neurochem Res* **25**, 1241–1244.
- Schroder W, Seifert G, Huttmann K, Hinterkeuser S & Steinhauser C (2002). AMPA receptor-mediated modulation of inward rectifier K^+ channels in astrocytes of mouse hippocampus. *Mol Cell Neurosci* **19**, 447–458.
- Seifert G, Huttmann K, Binder DK, Hartmann C, Wyczynski A, Neusch C & Steinhauser C (2009). Analysis of astroglial K^+ channel expression in the developing hippocampus reveals a predominant role of the Kir4.1 subunit. *J Neurosci* **29**, 7474–7488.
- Tanaka K, Watase K, Manabe T, Yamada K, Watanabe M, Takahashi K, Iwama H, Nishikawa T, Ichihara N, Kikuchi T, Okuyama S, Kawashima N, Hori S, Takimoto M & Wada K (1997). Epilepsy and exacerbation of brain injury in mice lacking the glutamate transporter GLT-1. *Science* **276**, 1699–1702.

- Teubner B, Michel V, Pesch J, Lautermann J, Cohen-Salmon M, Sohl G, Jahnke K, Winterhager E, Herberhold C, Hardelin JP, Petit C & Willecke K (2003). Connexin30 (Gjb6)-deficiency causes severe hearing impairment and lack of endocochlear potential. *Hum Mol Genet* **12**, 13–21.
- Theis M, Jauch R, Zhuo L, Speidel D, Wallraff A, Doring B, Frisch C, Sohl G, Teubner B, Euwens C, Huston J, Steinhauser C, Messing A, Heinemann U & Willecke K (2003). Accelerated hippocampal spreading depression and enhanced locomotory activity in mice with astrocyte-directed inactivation of connexin43. *J Neurosci* **23**, 766–776.
- Wallraff A, Kohling R, Heinemann U, Theis M, Willecke K & Steinhauser C (2006). The impact of astrocytic gap junctional coupling on potassium buffering in the hippocampus. *J Neurosci* **26**, 5438–5447.
- Wallraff A, Odermatt B, Willecke K & Steinhauser C (2004). Distinct types of astroglial cells in the hippocampus differ in gap junction coupling. *Glia* **48**, 36–43.
- Zhang X, Zhang J & Chen C (2009). Long-term potentiation at hippocampal perforant path-dentate astrocyte synapses. *Biochem Biophys Res Commun* **383**, 326–330.
- Zhou M, Xu G, Xie M, Zhang X, Schools GP, Ma L, Kimelberg HK & Chen H (2009). TWIK-1 and TREK-1 are potassium channels contributing significantly to astrocyte passive conductance in rat hippocampal slices. *J Neurosci* **29**, 8551–8564.

Additional information

Competing interests

The authors declare no competing interest.

Author contributions

All experiments were performed in the laboratory of ‘Neuroglial Interactions in Cerebral Physiopathology’ in the Center for Interdisciplinary Research in Biology at Collège de France. Conception and design of the experiments: N.R., J.S. Collection, analysis and interpretation of the data: J.S., U.P. and N.R. Drafting the article or revising it critically for important intellectual content: J.S., U.P. and N.R. All authors approved the final version of the manuscript.

Funding

This work was supported by grants from the HFSPO (Career Development Award), ANR (Programme Jeunes chercheurs and Programme Blanc Neurosciences), FRC (Fédération pour la Recherche sur le Cerveau), INSERM and La Pitié Salpêtrière hospital (Translational research contract) to N.R., from the doctoral school ‘Frontiers in Life Science’, Paris Diderot University, Bettencourt Schuller foundation, and FRM (Fondation pour la Recherche Médicale) doctoral fellowship to J.S., and from French Research Ministry and Deutsche Forschungsgemeinschaft postdoc fellowships to U.P.

Acknowledgements

We thank K. D. McCarthy for providing the $K_{ir4.1fl/fl};hGFAP-Cre$ mice, K. Willecke for providing the $Cx30^{-/-};Cx43fl/fl;hGFAP-Cre$ mice, and O. Chever and all members of the ‘Neuroglial Interactions in Cerebral Physiopathology’ laboratory for helpful discussions.

Author’s present address

Ulrike Pannasch: Ulrike Pannasch Neuroscience Research Center, Charité Universitätsmedizin, 10117 Berlin, Germany.